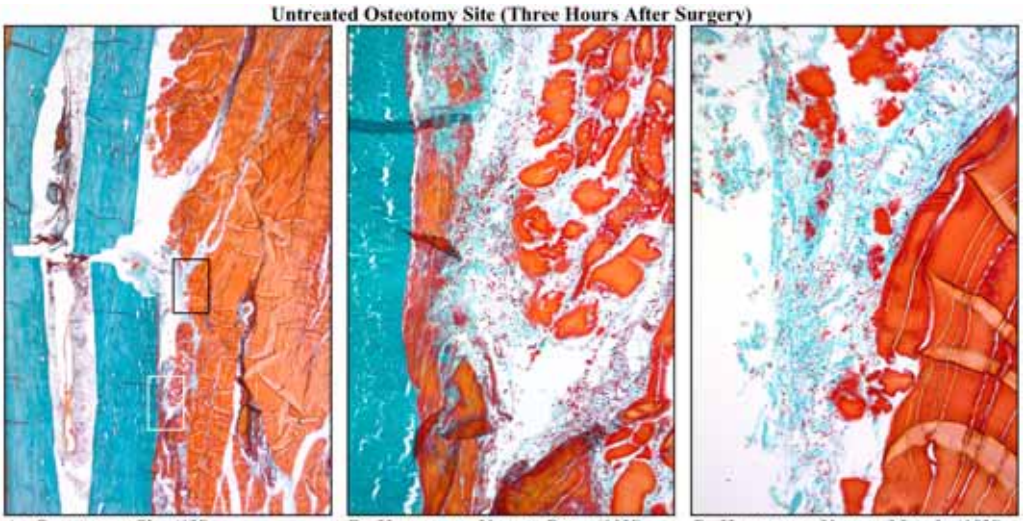

Fig. E-1

A, B, and *C:* Photomicrographs, made three hours after surgery, showing the histological appearance of the cellular infiltrate around an untreated nonhuman primate fibular osteotomy site. The hematoma, present at the osteotomy site adjacent to the bone *(B,* corresponding with the region within the white rectangle in *A)* and the muscle *(C,* corresponding with the region within the black rectangle in *A),* is composed primarily of both red and white blood cells, fibrin, and damaged muscle fibers (Goldner trichrome).

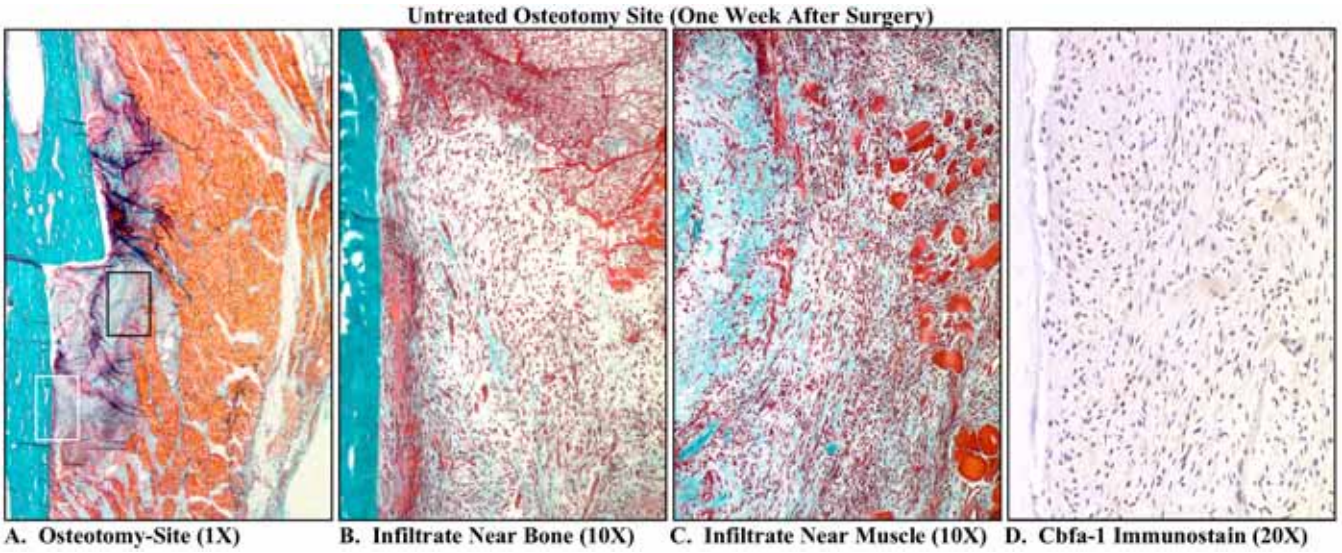

Fig. E-2

A through *D:* Photomicrographs, made one week after surgery, showing the histological appearance of the cellular infiltrate around an untreated nonhuman primate fibular osteotomy site. The dense cellular infiltrate, present at the osteotomy site adjacent to the bone *(B,* corresponding with the region within the white rectangle in *A)* and the muscle *(C,* corresponding with the region within the black rectangle in *A),* is composed primarily of spindle-shaped cells within the resolving hematoma/seroma (Goldner trichrome). Very few inflammatory cells are present at the osteotomy site at this time-point. The periosteal response within the white rectangle in *A* is shown in Figure E-3, *B*. A percentage of the spindle-shaped cells are presumed to be osteoblast precursors on the basis of the positive nuclear immunohistochemical stain (brown color) for core binding factor activity 1 (Cbfa-1) *(D,* hematoxylin counterstain).

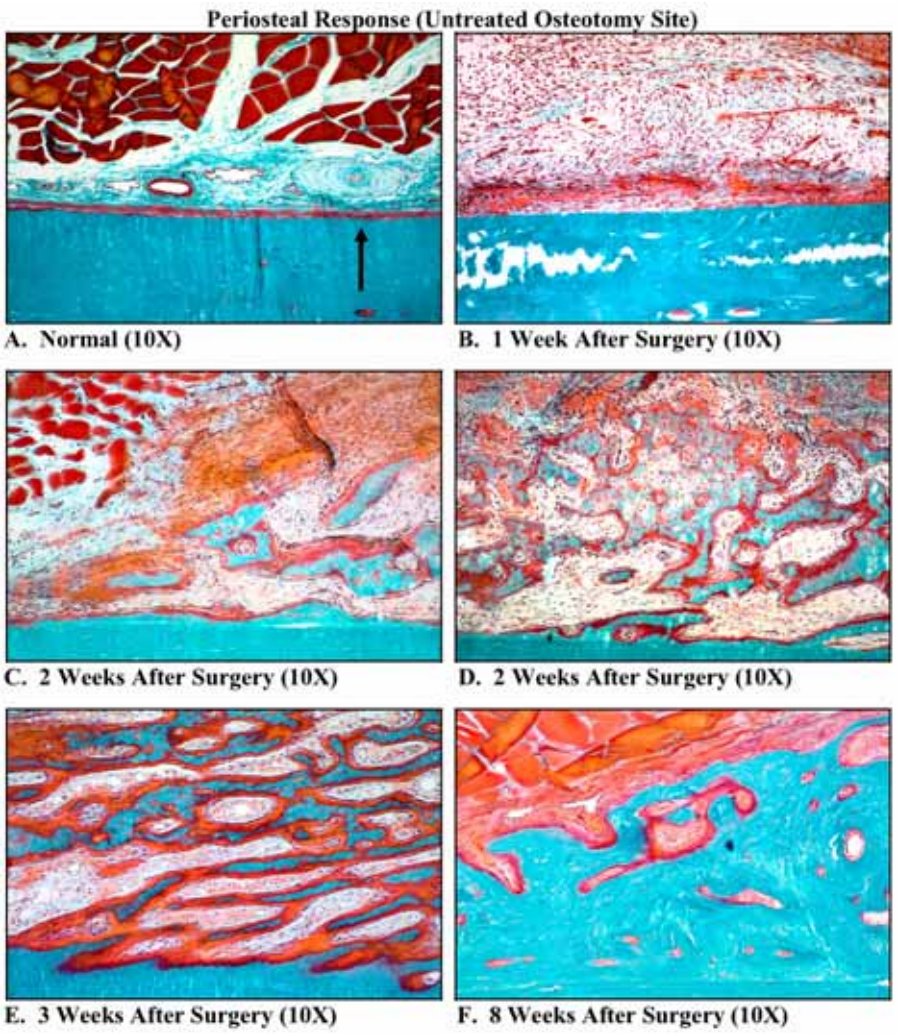

Fig. E-3

A through *F:* Photomicrographs showing the histological appearance of normal periosteum *(A)* and the periosteal response in an untreated nonhuman primate osteotomy site one week *(B,* corresponding with the region within the white rectangle in Figure E-2, *A),* two weeks *(C* and *D,* corresponding with the region within the white rectangle in Figure E-4, *B),* three weeks *(E,* corresponding with the region within the white rectangle in Figure E-5, *B),* and eight weeks *(F,* corresponding with the region within the white rectangle in Figure E-8, *B)* after surgery. A sensory Pacinian corpuscle is located adjacent to the normal periosteum (closed arrow in *A).* Although the primary mechanism of periosteal bone formation at two weeks appeared to be direct, there were regions within the periosteum in which a hybrid of direct and endochondral bone formation appeared to be occurring *(D).* Callus consolidation occurred by appositional bone filling in the spaces between the initial woven trabecular bone present at two weeks *(C* and *D)* during the subsequent three weeks *(E)* to eight weeks *(F)* after surgery (Goldner trichrome).

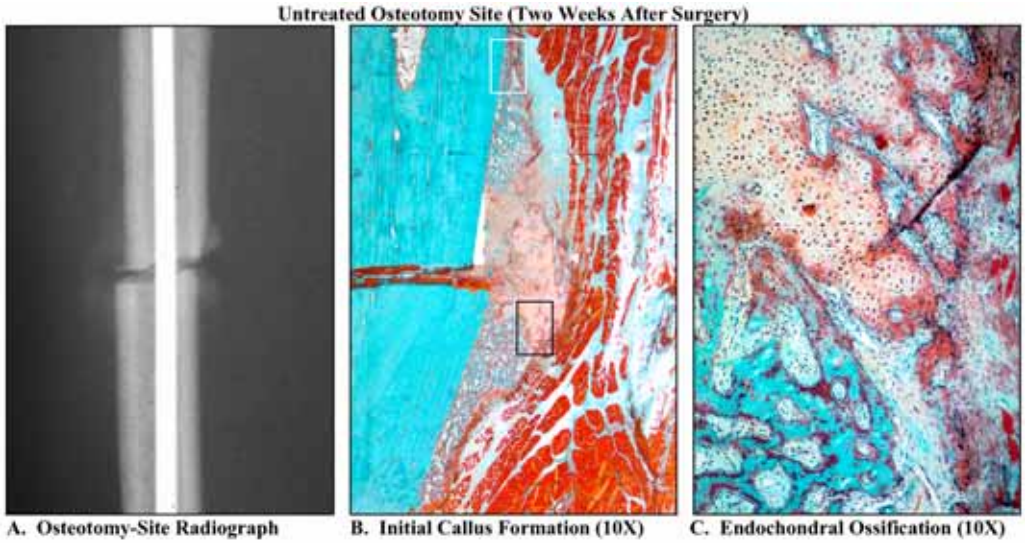

Fig. E-4

Radiograph *(A)* and photomicrographs *(B* and *C)* showing the appearance of an untreated nonhuman primate osteotomy site two weeks after surgery. Endochondral conversion of the soft callus is occurring at the periphery of the osteotomy site *(C,* corresponding with the region within the black rectangle in *B).* The periosteal response within the white rectangle in *B* is pictured in Figure E-3, *C* and *D.* The areas of new-bone formation in the region of endochondral conversion of the soft callus and the proximal and distal periosteal responses were associated with neovascularization *(C).* The central region of the cartilaginous soft callus was relatively avascular *(C)* (Goldner trichrome).

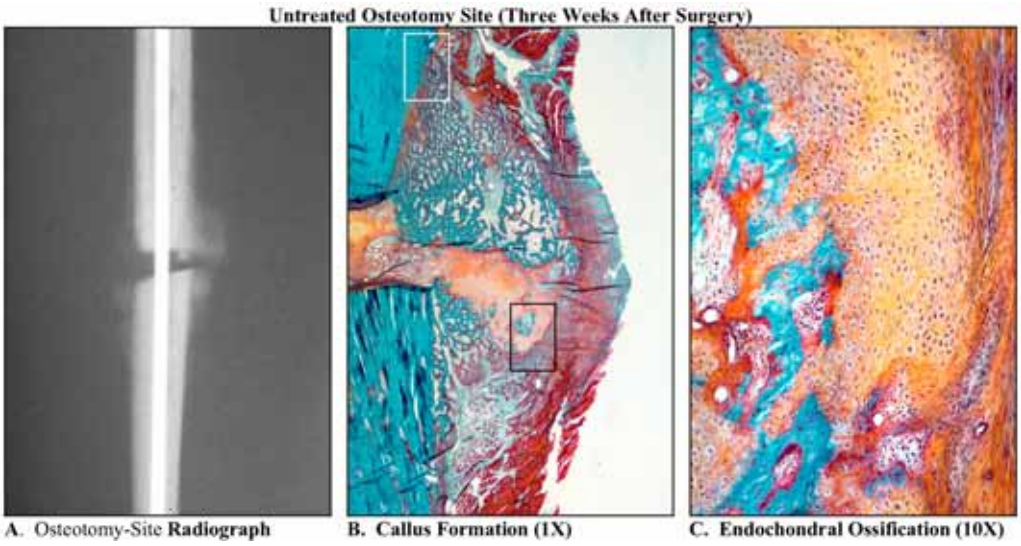

Fig. E-5

Radiograph *(A)* and photomicrographs *(B* and *C)* showing the appearance of an untreated nonhuman primate osteotomy site three weeks after surgery. Endochondral conversion of the soft callus continues to occur at the periphery of the osteotomy site *(C,* corresponding with the region within the black rectangle in *B).* The periosteal response within the white rectangle in *B* is pictured in Figure E-3, *E* (Goldner trichrome).

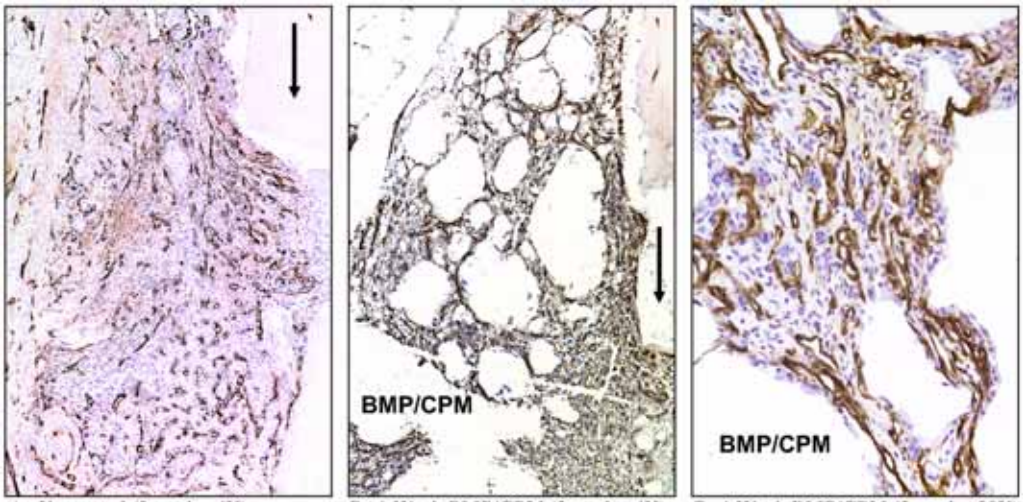

A. Untreated (3 weeks, 4X) B. 1 Week BMP/CPM (3 weeks, 4X) C. 1 Week BMP/CPM (3 weeks, 20X)

Fig. E-6

A, B, and *C:* Photomicrographs, made three weeks after surgery, showing the histological appearance of neovascularization as demonstrated by immunohistochemical staining for type-IV collagen in the vessel walls (brown stain) in an untreated nonhuman primate fibular osteotomy site *(A)* and in an osteotomy site that had been treated with rhBMP-2/calcium phosphate matrix one week after surgery *(B* and *C).* The closed arrows in *A* and *B* indicate the osteotomy sites. There was an increase in neovascularization associated with rhBMP-2/calcium phosphate matrix treatment at both two and three weeks after surgery (hematoxylin counterstain).

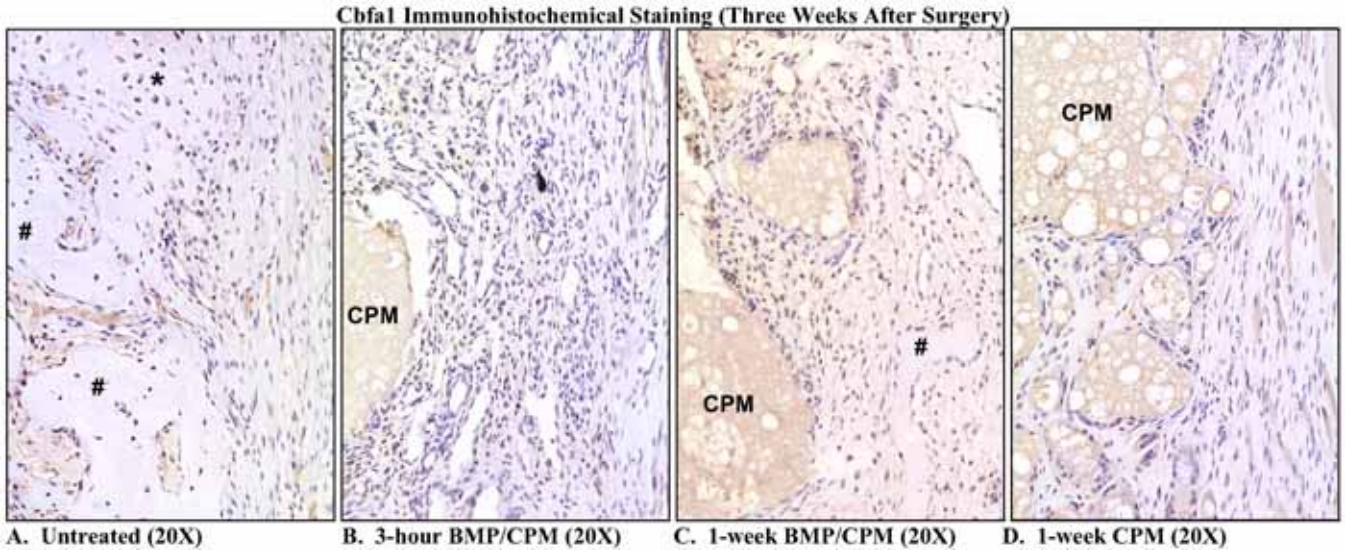

Fig. E-7

Photomicrographs, made three weeks after surgery, showing the histological appearance of immunohistochemical nuclear staining for Cbfa1 (brown color) in the cellular infiltrate in an untreated nonhuman primate fibular osteotomy site in the region of endochondral conversion of the cartilaginous callus *(A)* and in osteotomy sites treated with rhBMP-2/calcium phosphate matrix at three hours after surgery *(B),* with rhBMP-2/calcium phosphate matrix administered one week after surgery *(C)*, and with calcium phosphate matrix alone administered one week after surgery *(D)*. The region depicted in *A* is undergoing endochondral conversion of the cartilaginous callus (*) to bone (#). The regions depicted in *B, C,* and *D* are at the periphery of the osteotomy sites at the interface between the calcium phosphate matrix granules and the surrounding soft tissues. Direct bone formation in this region can be seen in *C* (#) (hematoxylin counterstain).

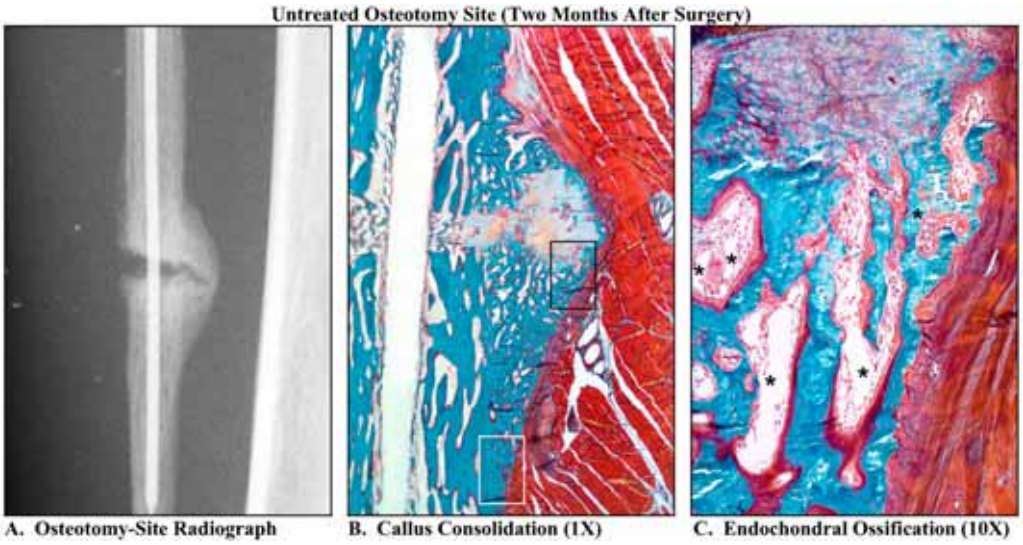

Fig. E-8

Radiograph *(A)* and photomicrographs *(B* and *C),* made two months after surgery, showing the appearance of an untreated nonhuman primate osteotomy site. Endochondral conversion of the soft callus continues to occur at the periphery of the osteotomy site *(C,* corresponding with the region within the black rectangle in *B)* in association with neovascularization (*****). Considerable mineralization of the cartilaginous callus is present adjacent to the region of endochondral conversion. The periosteal response within the white rectangle in *B* is shown in Figure E-3, *F.* There is evidence of cortical remodeling, presumably in response to the increased cross-sectional area of the combined cortex and callus and to stress-shielding due to the presence of the Kirschner wire (Goldner trichrome).

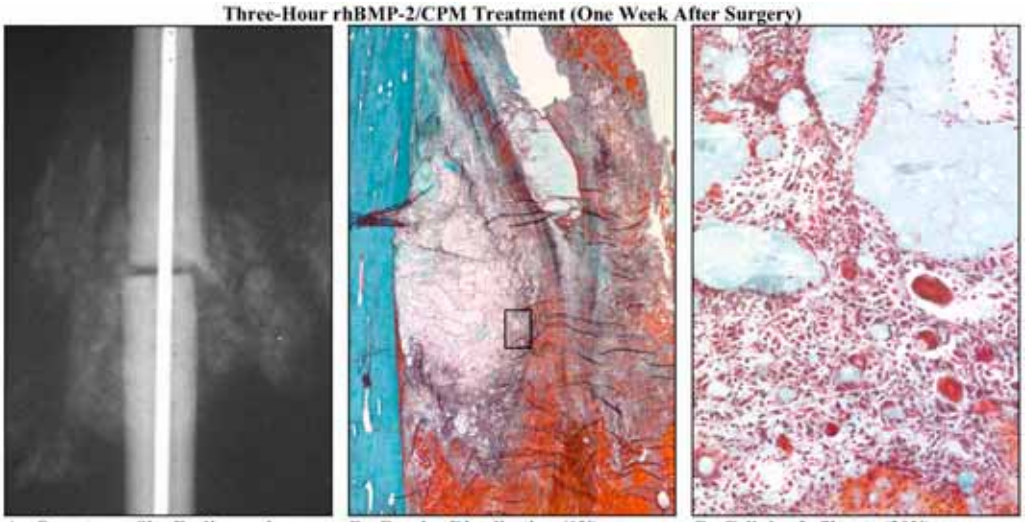

Fig. E-9

Radiograph *(A)* and photomicrographs *(B* and *C),* made one week after surgery, showing the appearance of a nonhuman primate osteotomy site that had been treated with rhBMP-2/calcium phosphate matrix three hours after surgery. Dense cellular infiltrate surrounding the rhBMP-2/calcium phosphate matrix granules at the periphery of the osteotomy site consists of spindle-shaped cells, macrophages, and multinucleated cells *(C,* corresponding to the region within the closed rectangle in *B)* (Goldner trichrome).

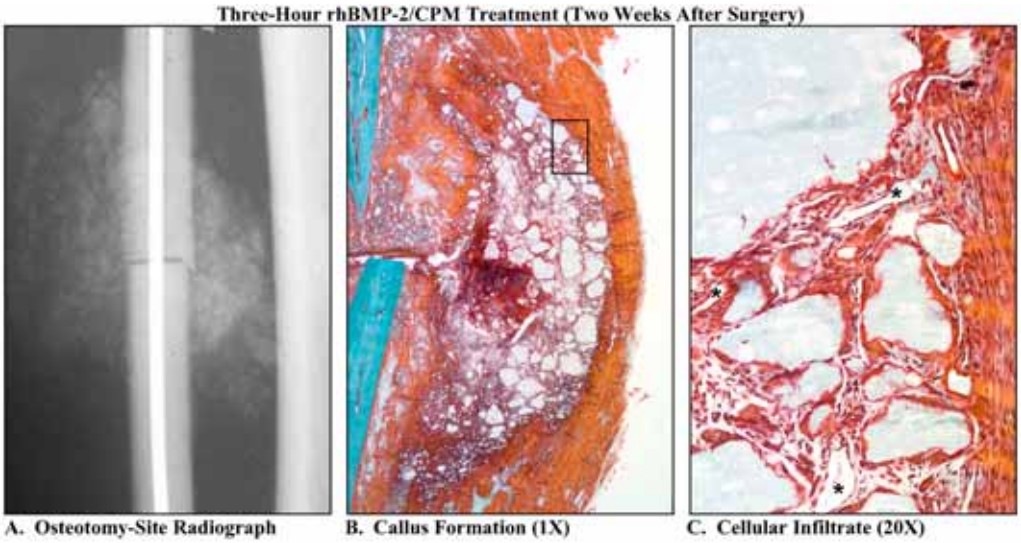

Fig. E-10

Radiograph *(A)* and photomicrographs *(B* and *C),* made two weeks after surgery, showing the appearance of a nonhuman primate osteotomy site that had been treated with rhBMP-2/calcium phosphate matrix three hours after surgery. The majority of the initial hematoma/seroma had resolved by this time-point. The periosteal new-bone formation proximal and distal to the osteotomy site was similar to the response observed in the untreated osteotomy sites. However, the size of the centrally located cartilaginous callus was reduced because of the presence of the calcium phosphate matrix granules as compared with the findings in the untreated osteotomy site at this time-point. Cellular infiltrate surrounding the rhBMP-2/calcium phosphate matrix granules at the periphery of the osteotomy site consists of spindle-shaped cells, macrophages, multinucleated giant cells, and osteoclasts (Fig. E-11) and newly forming blood vessels (*) *(C,* region within the rectangle in *B)* (Goldner trichrome).

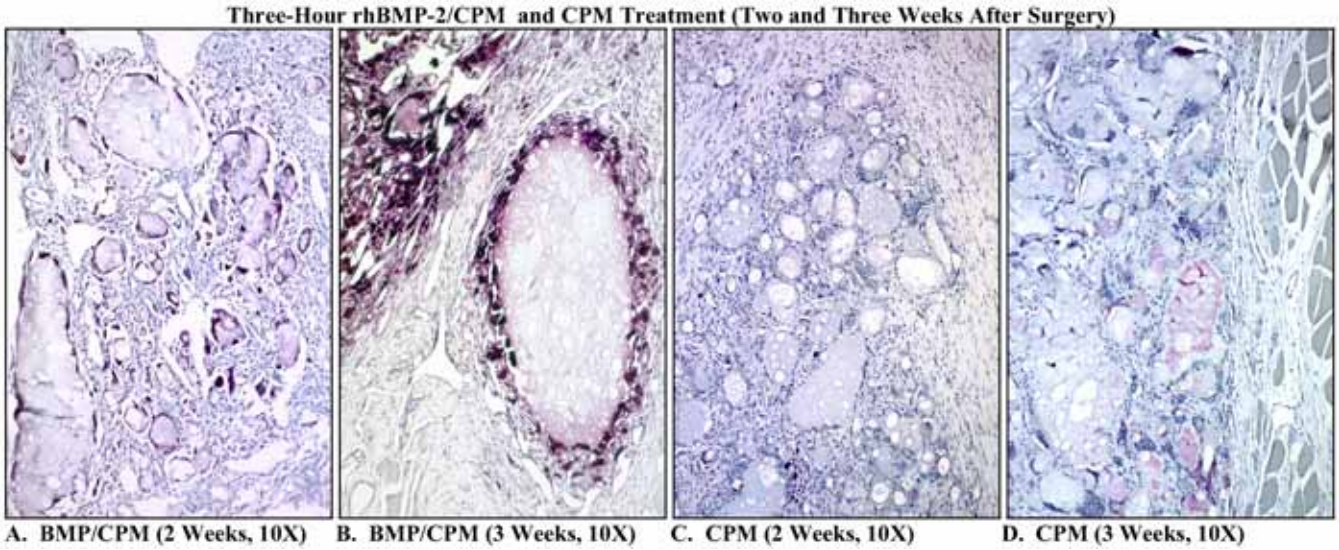

Fig. E-11

Photomicrographs, made two weeks *(A* and *C)* and three weeks *(B* and *D)* after surgery, showing the histological appearance of calcium phosphate matrix resorption in nonhuman primate fibular osteotomy sites that had been treated with rhBMP-2/calcium phosphate matrix *(A* and *B)* or with calcium phosphate matrix alone *(C* and *D)* at three hours after surgery. *A:* At two weeks, mild-intensity TRAP-positive-stained multinucleated giant cells were present, engulfing the smaller-sized particles and, to a lesser extent, intense TRAP-positive-stained osteoclasts were observed resorbing the surfaces of larger-sized particles of rhBMP-2/calcium phosphate matrix. *B:* At three weeks, the majority of multinucleated cells observed resorbing the rhBMP-2/calcium phosphate matrix granules were intense TRAP-positive-stained osteoclasts. *C:* At two weeks, the dispersed calcium phosphate matrix granules were surrounded by a dense infiltrate made up primarily of macrophages and TRAP-negative-stained multinucleated giant cells. *D:* At three weeks, the majority of the multinucleated giant cells surrounding the calcium phosphate matrix granules were also TRAP-negative-stained (hematoxylin counterstain).

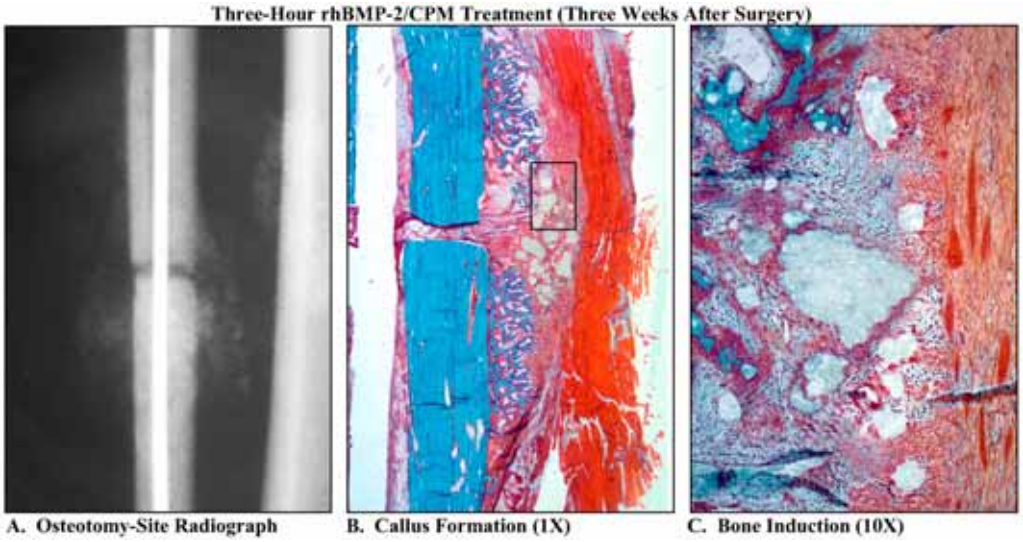

Fig. E-12

Radiograph *(A)* and photomicrographs *(B* and *C),* made three weeks after surgery, showing the appearance of a nonhuman primate osteotomy site that had been treated with rhBMP-2/calcium phosphate matrix at three hours after surgery. Periosteal bone formation is ongoing proximal and distal to the osteotomy site *(B).* New-bone formation and neovascularization are visible in association with a dense infiltrate of spindle-shaped cells corresponding to the Cbfa-1 positive cells in Figure E-7, *B* and neovascularization between the calcium phosphate matrix granules within the osteotomy site *(C,* region within the rectangle in *B).* Endochondral bone formation at the osteotomy site appeared to be reduced compared with that in untreated osteotomy sites at this same time-point because of the presence of the calcium phosphate matrix granules. Multinucleated osteoclasts corresponding to the TRAP-positive-stained cells in Figure E-11, *C* can be seen resorbing the calcium phosphate matrix granules *(C)* (Goldner trichrome).

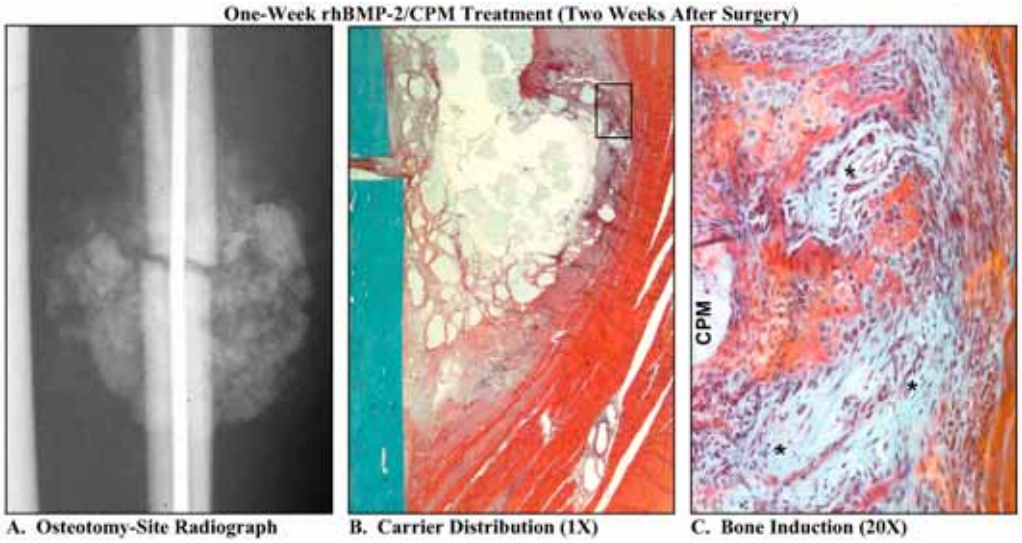

Fig. E-13

Radiograph *(A)* and photomicrographs *(B* and *C),* made two weeks after surgery, showing the appearance of a nonhuman primate osteotomy site that had been treated with rhBMP-2/calcium phosphate matrix one week after surgery. The calcium phosphate matrix granules were larger and were associated with less seroma as compared with the three-hour rhBMP-2/calcium phosphate matrix-treated osteotomy sites at the same time-point (Fig. E-10). A combination of direct and endochondral bone formation, as well as newly forming blood vessels (*), are occurring adjacent to the rh-BMP-2/calcium phosphate matrix granules (CPM) at the periphery of the osteotomy site *(C,* region within the rectangle in *B).* As was the case in the osteotomy sites that had been treated with rhBMP-2/calcium phosphate matrix administered at three hours after surgery, there was a decrease in the amount of cartilaginous callus present at the osteotomy site as compared with the untreated osteotomy sites at the same time-point (Fig. E-4). The majority of the multinucleated cells resorbing the calcium phosphate matrix granules were intense TRAP-positive-stained osteoclasts and giant cells (Fig. E-14, *A*) (Goldner trichrome).

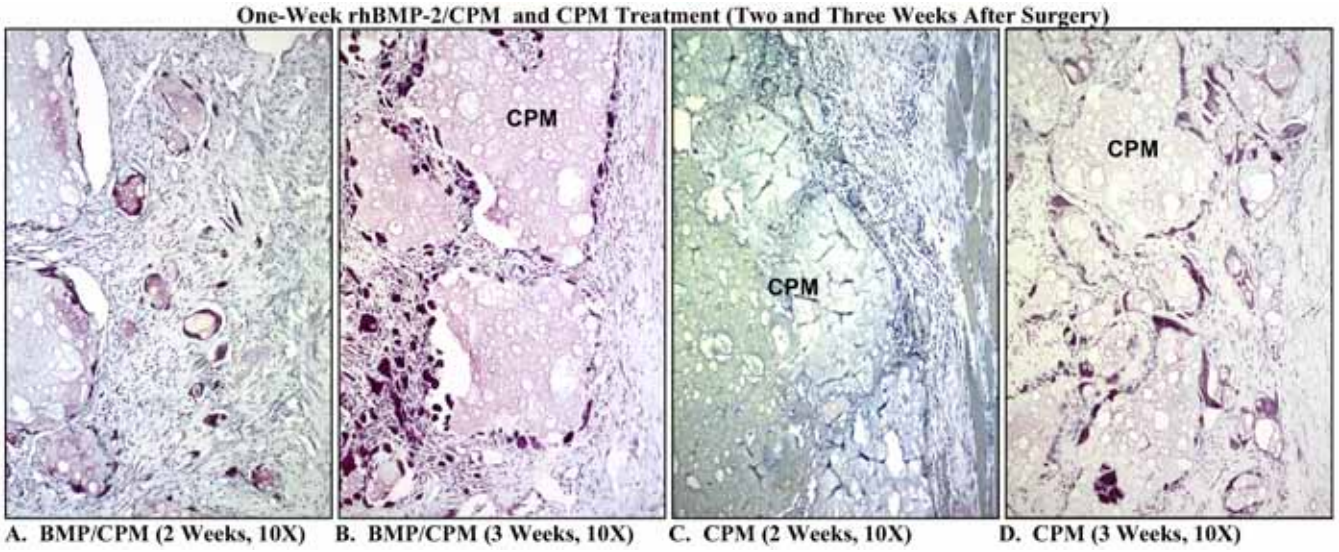

Fig. E-14

Photomicrographs, made two weeks *(A* and *C)* and three weeks *(B* and *D)* after surgery, showing the histological appearance of calcium phosphate matrix resorption in nonhuman primate fibular osteotomy sites that had been treated with rhBMP-2/calcium phosphate matrix *(A* and *B)* or with calcium phosphate matrix alone (*C* and *D*) at one week after surgery. The majority of the multinucleated cells resorbing the rhBMP-2/calcium phosphate matrix granules were intense TRAP-positive-stained osteoclasts and giant cells at two weeks and three weeks *(A* and *B).* The majority of the multinucleated giant cells resorbing calcium phosphate matrix were TRAP-negative-stained giant cells at two and three weeks *(C* and *D)* (hematoxylin counterstain).

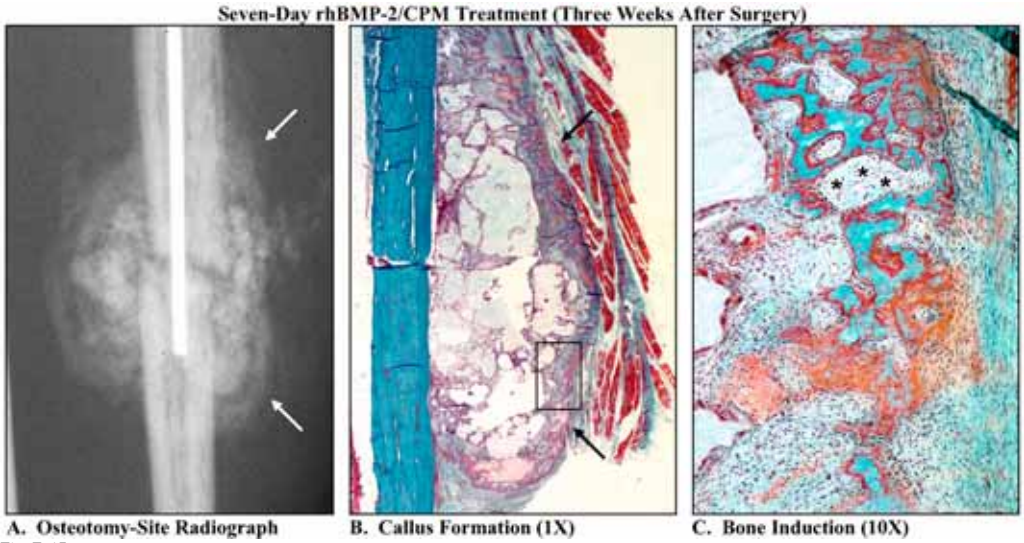

Fig. E-15

Radiograph *(A)* and photomicrographs *(B* and *C)*, made three weeks after surgery, showing the appearance of a nonhuman primate osteotomy site that had been treated with rhBMP-2/calcium phosphate matrix at one week after surgery. The radiodense halo visible on the radiograph *(A,* arrows) surrounding the residual calcium phosphate matrix corresponds to new-bone formation visible in the histological section *(B,* arrows) at the periphery of the osteotomy site adjacent to calcium phosphate matrix granules. New-bone formation at the periphery of the osteotomy site appears to be occurring primarily via a direct pathway without a cartilage intermediate *(C,* corresponding with the region within the rectangle in *B).* Small regions of endochondral ossification were also observed along the periphery of the osteotomy site. New-bone formation was associated with a dense infiltrate of spindle-shaped cells corresponding to the Cbfa-1-positive cells in Figure E-7, *C* and neovascularization (*) corresponding to the vessels stained for type IV collagen in Figure E-6, *B* and *C*. Osteoclasts were observed resorbing the residual calcium phosphate matrix granules (see Fig. E-14, *B*) (Goldner trichrome).

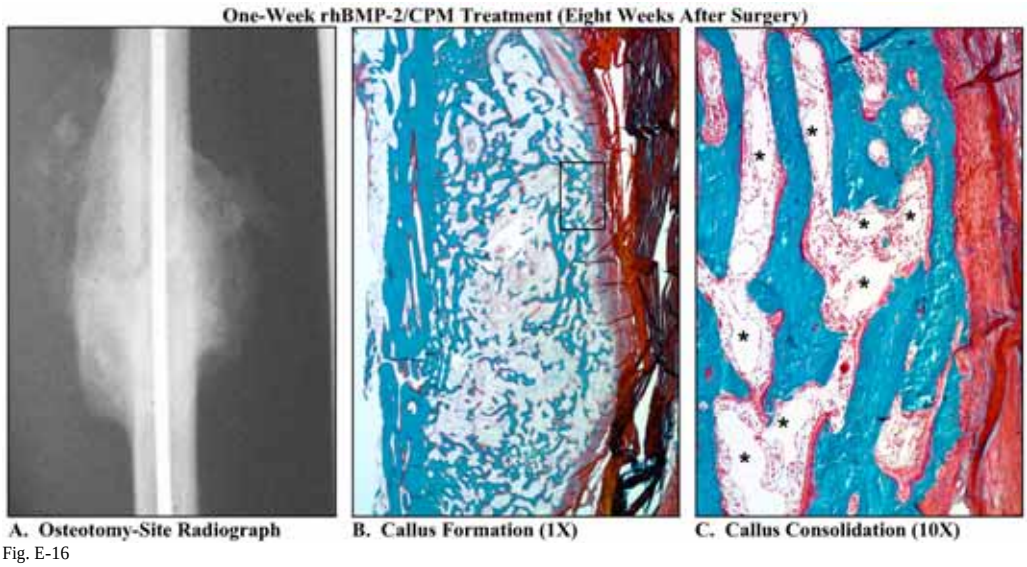

Fig. E-16

Radiograph *(A)* and photomicrographs *(B* and *C),* made eight weeks after surgery, showing the appearance of a nonhuman primate osteotomy site that had been treated with rhBMP-2/calcium phosphate matrix one week after surgery. Appositional bone formation on newly formed trabeculae is continuing to fill in the marrow spaces between trabeculae both within and at the periphery of the osteotomy site *(C,* corresponding with the region within the rectangle in *B).* Numerous new blood vessels (*) are present within the activated marrow spaces. As was the case in the untreated osteotomy sites at this time-point (Fig. E-8), there is evidence of cortical remodeling, presumably in response to the increased cross-sectional area of the combined cortex and callus and to stress-shielding due to the presence of the Kirschner wire (Goldner trichrome).

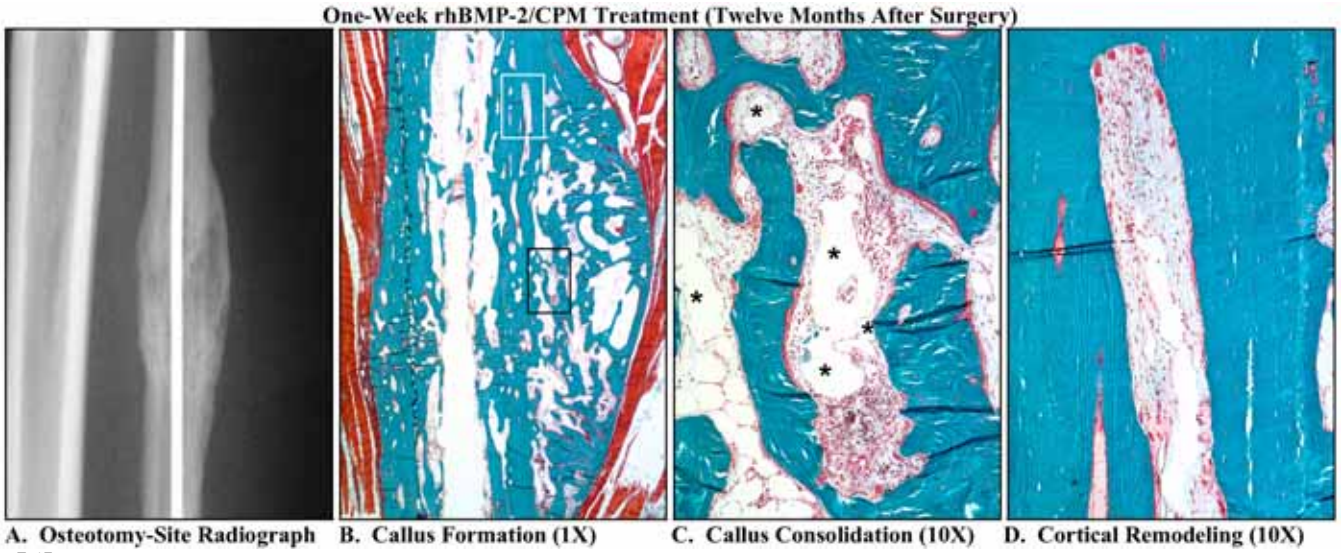

Fig. E-17

Radiograph *(A)* and photomicrographs *(B, C,* and *D),* made twelve months after surgery, showing the appearance of a nonhuman primate osteotomy site that had been treated with rhBMP-2/calcium phosphate matrix one week after surgery. Appositional lamellar bone formation on newly formed trabeculae is continuing to fill in the marrow spaces between trabeculae within the osteotomy site callus *(C,* corresponding with the region within the black rectangle in *B).* Numerous new blood vessels (*) are still present within the activated marrow spaces as well as adipose cells. The presence of osteoclasts indicates ongoing remodeling of the original cortex *(D,* corresponding with the region within the white rectangle in *B)* (Goldner trichrome).

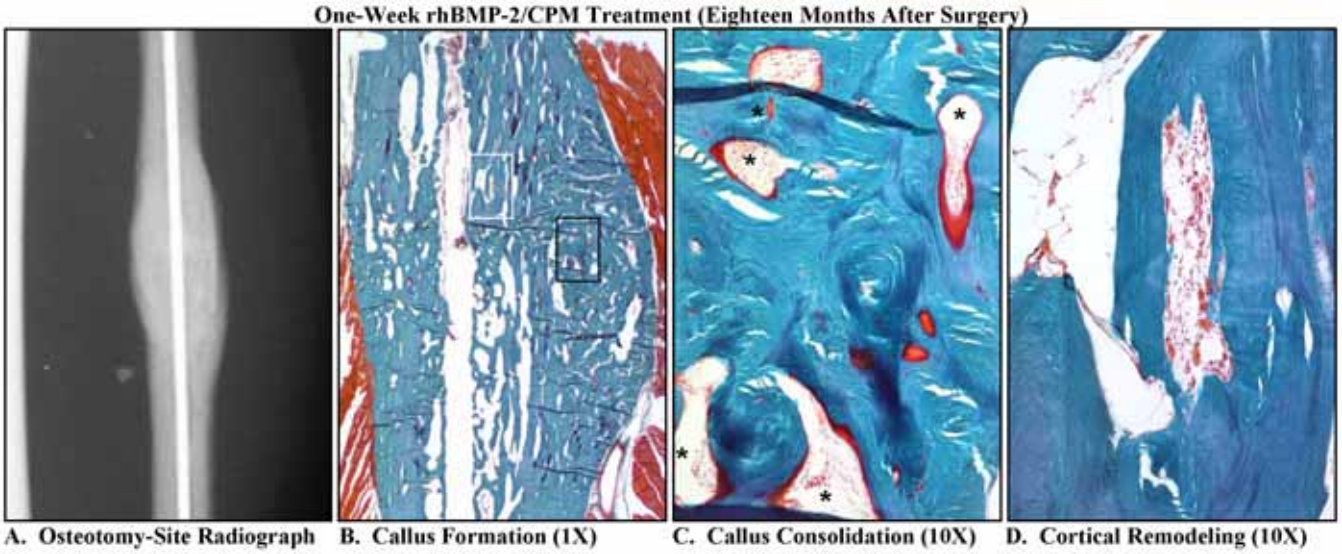

Fig. E-18

Radiograph *(A)* and photomicrographs *(B, C,* and *D),* made eighteen months after surgery, showing the appearance of a nonhuman primate osteotomy site that had been treated with rhBMP-2/calcium phosphate matrix one week after surgery. Appositional lamellar bone formation on newly formed trabeculae is continuing to fill in the marrow spaces between trabeculae within the osteotomy site callus *(C,* corresponding with the region within the black rectangle in *B).* Numerous new blood vessels (*) are still present within the activated marrow spaces as well as adipose cells. Resorption of the original cortex continues *(D,* corresponding with the region within the white rectangle in *B)* (Goldner trichrome).

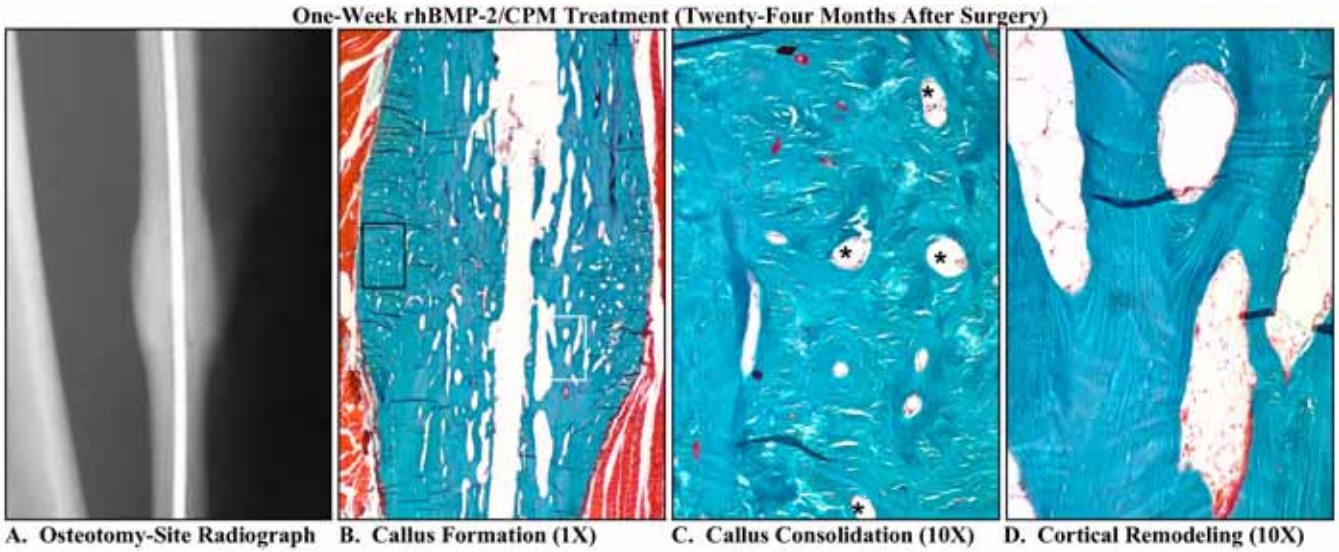

Fig. E-19

Radiograph *(A)* and photomicrographs *(B, C,* and *D),* made twenty-four months after surgery, showing the appearance of a nonhuman primate osteotomy site that had been treated with rhBMP-2/calcium phosphate matrix one week after surgery. Appositional lamellar bone has largely filled in the marrow spaces between trabeculae within the osteotomy site callus *(C,* region within the black rectangle in *B).* Blood vessels (*) are still present within the narrowed marrow spaces, and the randomly aligned lamellar pattern is apparent (Fig. 3). Resorption of the original cortex with the establishment of normal marrow elements is almost completed *(D,* corresponding with the region within the white rectangle in *B)* (Goldner trichrome).

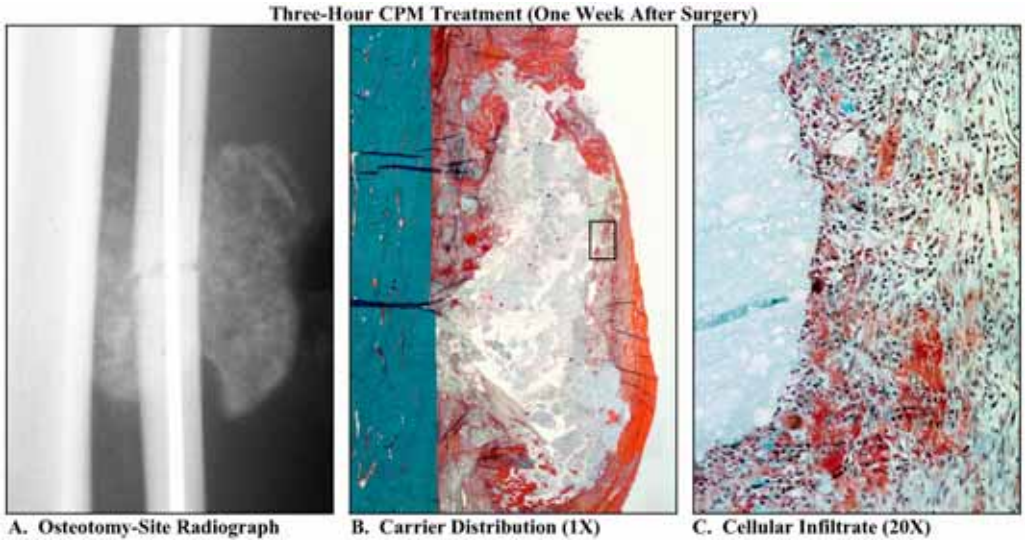

Fig. E-20

Radiograph *(A)* and photomicrographs *(B* and *C),* made one week after surgery, showing the appearance of a nonhuman primate osteotomy site that had been treated with calcium phosphate matrix three hours after surgery. Mixed cellular infiltrate including macrophages, monocytes, lymphocytes, red blood cells, and spindle-shaped cells surround the calcium phosphate matrix granules at the periphery of the osteotomy site *(C,* corresponding with the region within the rectangle in *B)* (Goldner trichrome).

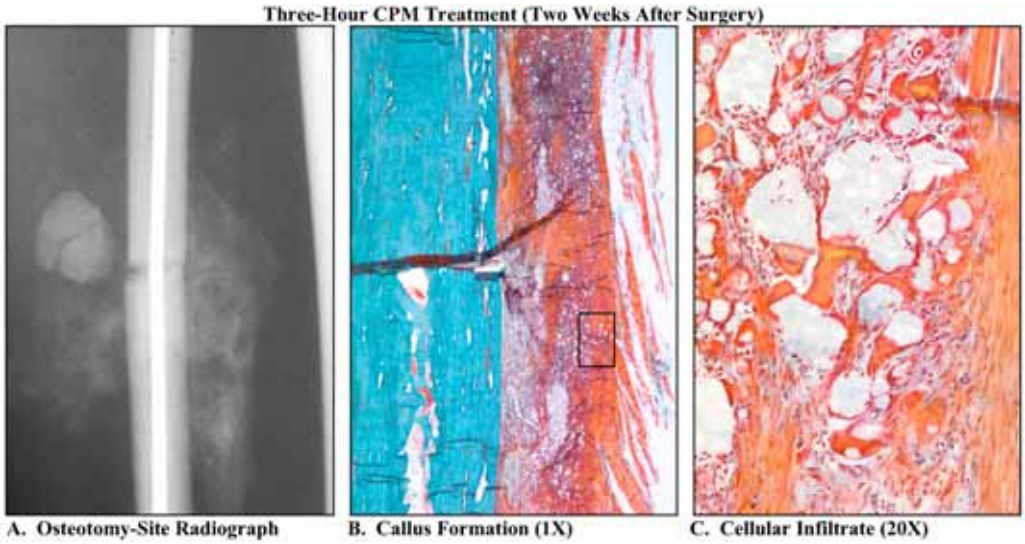

Fig. E-21

Radiograph *(A)* and photomicrographs *(B* and *C),* made two weeks after surgery, showing the appearance of a nonhuman primate osteotomy site that had been treated with calcium phosphate matrix three hours after surgery. Cellular infiltrate surrounding the dispersed calcium phosphate matrix granules at the periphery of the osteotomy site consists mainly of macrophages, multinucleated cells engulfing and resorbing the carrier (Fig. E-11), and some spindle-shaped cells *(C,* corresponding with the region within the rectangle in *B).* As was the case with rhBMP-2/calcium phosphate matrix treatment, the centrally located cartilaginous callus was reduced in size because of the presence of the calcium phosphate matrix granules in this location. Periosteal new bone was forming proximal and distal to the osteotomy site at two weeks after surgery (Goldner trichrome).

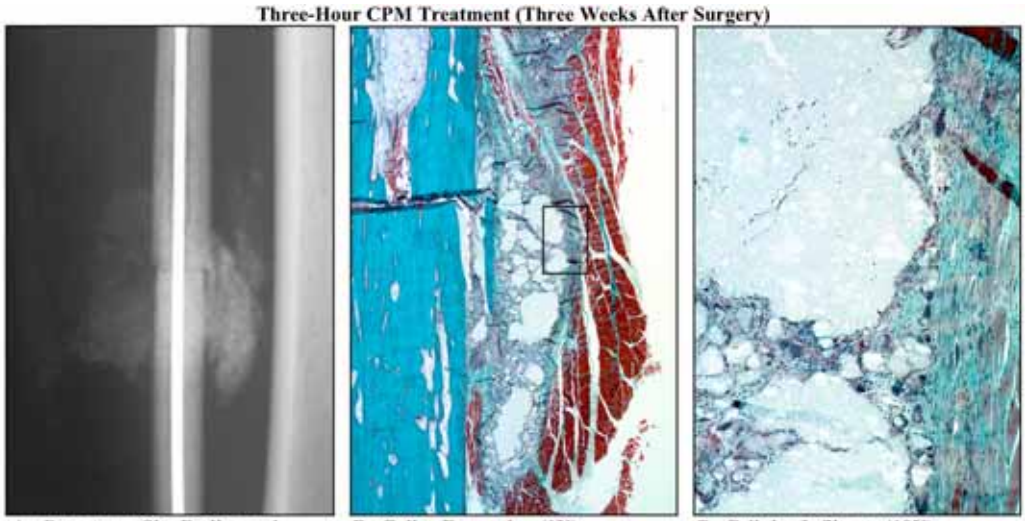

Fig. E-22

Radiograph *(A)* and photomicrographs *(B* and *C),* made three weeks after surgery, showing the appearance of a nonhuman primate osteotomy site that had been treated with calcium phosphate matrix three hours after surgery. Cellular infiltrate surrounding the calcium phosphate matrix granules at the periphery of the osteotomy site consists mainly of macrophages and multinucleated cells engulfing and resorbing the carrier (Fig. E-11) *(C,* corresponding with the region within the rectangle in *B).* There is no evidence of peripheral bone formation associated with the calcium phosphate matrix granules at this time-point (Goldner trichrome).

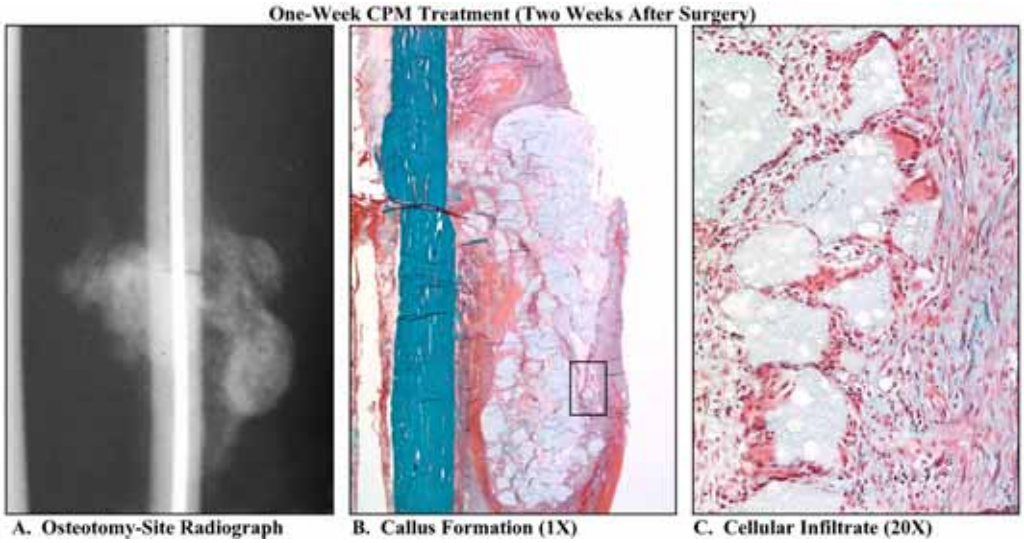

Fig. E-23

Radiograph *(A)* and photomicrographs *(B* and *C),* made two weeks after surgery, showing the appearance of a nonhuman primate osteotomy site that had been treated with calcium phosphate matrix one week after surgery. As was the case with the rhBMP-2/calcium phosphate matrix administered one week after surgery, there was less dispersion of the calcium phosphate matrix administered at one week than there was of the calcium phosphate matrix administered three hours after surgery at this same time-point (Fig. E-21). Cellular infiltrate surrounding the calcium phosphate matrix granules at the periphery of the osteotomy site consists mainly of macrophages, a smaller number of TRAP-negative-stained multinucleated cells (Fig. E-14, *C*) engulfing and resorbing the carrier compared with the three-hour calcium phosphate matrix treatment at the same time-point, and spindle-shaped cells *(C,* corresponding with the region within the rectangle in *B).* Periosteal new-bone formation was present proximal and distal to the osteotomy site (Goldner trichrome).

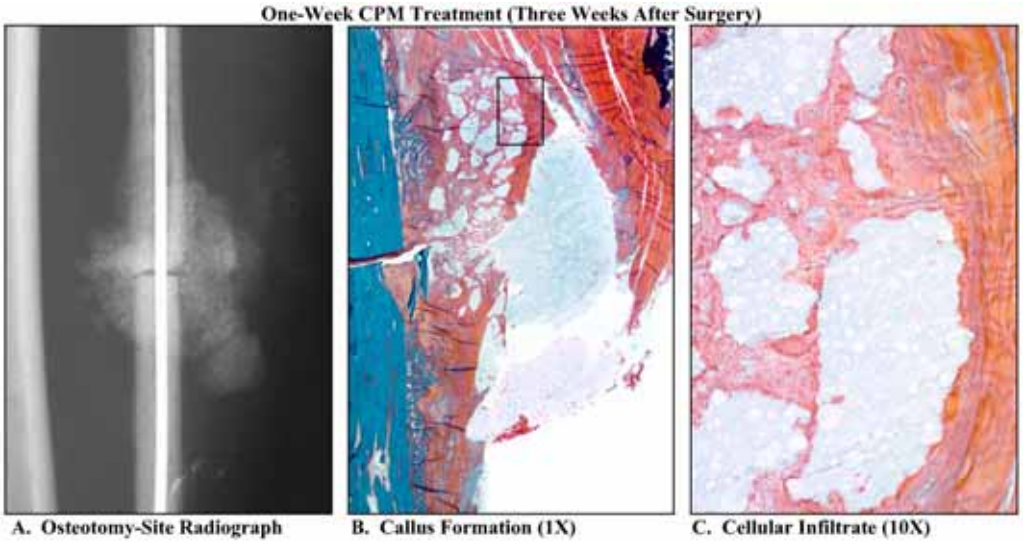

Fig. E-24

Radiograph *(A)* and photomicrographs *(B* and *C),* made three weeks after surgery, showing the appearance of a nonhuman primate osteotomy site that had been treated with calcium phosphate matrix one week after surgery. Cellular infiltrate surrounding the calcium phosphate matrix granules at the periphery of the osteotomy site consists mainly of macrophages, multinucleated cells engulfing and resorbing the carrier, and spindle-shaped cells *(C,* corresponding with the region within the rectangle in *B).* Some of the multinucleated giant cells exhibited moderate TRAP-positive-staining, and occasional heavy TRAP-positive-stained osteoclasts were observed on the surfaces of the calcium phosphate matrix granules (Fig. E-14, *D*). The majority of the spindle-shaped cells contained negative nuclear immunohistochemical stain for Cbfa1 (Fig. E-7). The centrally located cartilaginous callus remained reduced. Periosteal new-bone formation proximal and distal to the osteotomy site increased compared with earlier time-points. There is no evidence of peripheral bone formation associated with the calcium phosphate matrix granules at this time-point (Goldner trichrome).

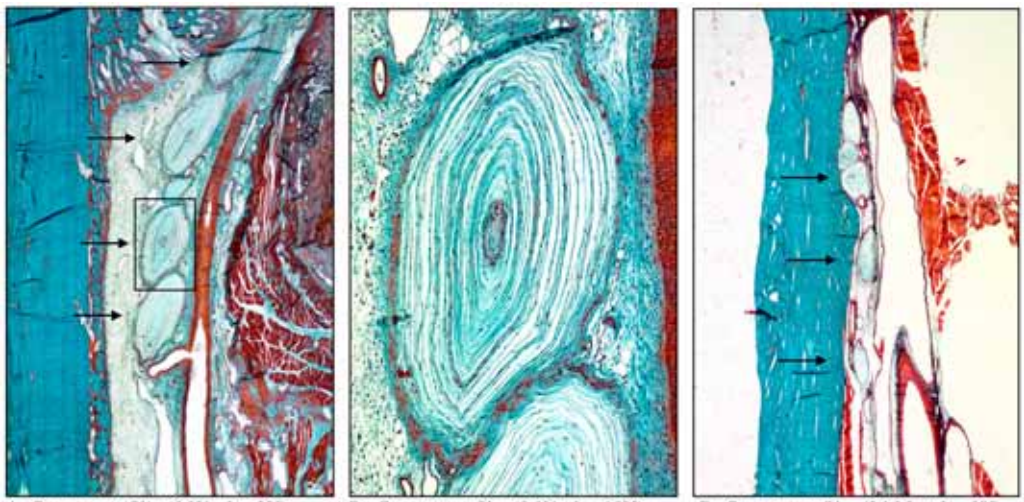

Fig. E-25

A: Proliferation and hypertrophy of sensory Pacinian corpuscles (arrows) associated with the periosteum near osteotomy sites were observed in approximately 30% of the operated fibulae three weeks after surgery. These clusters of receptors were found in all of the groups in this study, including the untreated osteotomy sites. *B:* Higher magnification of the Pacinian corpuscle located within the rectangle in *A,* demonstrating the increase in size relative to normal (Fig. E-3, *A). C:* Increased numbers of Pacinian corpuscles (arrows) persisted adjacent to remodeling osteotomy sites at twenty-four months after surgery (Goldner trichrome).